

K. HABERL\*, W. K. KRAJEWSKI\*\*, P. SCHUMACHER\*,\*\*\*

## MICROSTRUCTURAL FEATURES OF THE GRAIN-REFINED SAND CAST AlZn20 ALLOY

### CECHY MIKROSTRUKTURY ZMODYFIKOWANEGO STOPU AlZn20 ODLANEGO DO FORMY PIASKOWEJ

The influence of various titan-containing grain refiners on an AlZn20-alloy was examined using thermal analysis, light microscopy and scanning electron microscopy, and evaluation of grain size. The aim of this study was to determine microstructural features. The study showed that the magnitude of the melts undercooling, initial temperatures of primary nucleation and grain refinement are highly influenced by the grain refiner used.

*Keywords:* AlZn-alloys, AlZn20, grain refinement, thermal analysis, undercooling, primary nucleation temperature

W pracy badano wpływ różnych zapraw modyfikujących, zawierających tytan, na strukturę stopu AlZn20. W badaniach stosowano techniki analizy termicznej, mikroskopii świetlnej i elektronowej oraz analizę wielkości ziarna. Badania wykazały, że wielkość przechłodzenia i cechy struktury stopu zmodyfikowanego silnie zależą od rodzaju użytego modyfikatora.

## 1. Introduction

The casting production of Al-alloys compared with Fe-based alloys is small in the European Union, just as in the world [1]. For economical and ecological reasons, it is worthwhile to replace a portion of Fe-based castings with light metal alloys like AlZn. AlZn-alloys are economic to use because of their low melting point, low heating energy cost during production and their low weight that saves energy during transport applications. To develop AlZn-alloys with high mechanical properties, an adequate melt treatment is necessary, including an optimized grain-refinement.

## 2. Experimental

A study on the influence of various grain refiners on an AlZn20-alloy was performed. Microstructural features were examined with thermal analyses, investigations with light microscope (LM) and scanning electron microscope (SEM) and determination of grain size. Damping behaviour was also studied; the results of this study are part of reference [2].

### Initial alloy and grain refiners

The major alloying element of the initial alloy was Zn. The exact composition of the initial alloy was measured by chemical analysis (ICP-OES VARIAN Vista MPX and Sartorius ED224S) at the Austrian Foundry Research Institute: Zn 20,50 wt-%, Si < 0,02 wt-% and Cu, Fe, Mn, Mg, Cr, Ni, Sn, Ti < 0,01 wt-%. The used grain refiners were AlTi5B1, AlTi3C0,15, ZnTi4 and ZnAl20Ti3.

### Manufacturing of samples

Casting was performed at the Faculty of Foundry Engineering, AGH Krakow. The AlZn20 was melted in a resistance furnace (Czylok, Piec Tygłowy PT 12/1300) at 740°C. It was purged with Ar to reduce the hydrogen level. After adding each grain refiner into a crucible with AlZn20-alloy, the melt was stirred with a glass stirrer for 1 minute in order to produce a uniform melt concentration. The added amounts of grain refiner resulted in Ti-contents in the melt of 417-503 ppm. These samples were cast in a sand mould (bentonite bonded silica sand).

\* CHAIR OF CASTING RESEARCH, METALLURGY DEPARTMENT, UNIVERSITY OF LEOBEN, FRANZ-JOSEF-STR. 18, 8700 LEOBEN, AUSTRIA

\*\* FACULTY OF FOUNDRY ENGINEERING, AGH UNIVERSITY OF SCIENCE & TECHNOLOGY, REYMONTA 23 STR., 30-059 KRAKOW, POLAND

\*\*\* AUSTRIAN FOUNDRY RESEARCH INSTITUTE, PARKSTR. 21, 8700 LEOBEN, AUSTRIA

### Thermal analysis

All thermal analyses for determination of undercooling were performed at the Faculty of Foundry Engineering, AGH Krakow. The samples were located in a crucible (Noltina, AG Graphite) and molten in the above described resistance furnace. For the thermal analysis, the crucibles were taken out of the furnace and a thermocouple type K NiAl-NiCr was placed in the middle of the crucible filled with melt (see Figure 1a). To record the thermal analysis, the Agilent Technologies 34970A Data Acquisition Switch Unit and the computer software Agilent Bench Link Data Logger was used. Figure 1b shows the used units.

The undercooling relative to the liquidus temperature ( $\Delta T$ ) of all alloys and the initial temperatures of primary nucleation ( $T_n$ ) of all alloys with the exception of AlZn20+ZnTi4, due to poor results in undercooling and grain size examination, were calculated to show the effectiveness of the various grain refiners.

$T_n$  results from the differentiated thermal analysis curve provide information about the first nucleation events.  $T_n$  was expected to increase with the addition of a grain refiner [3-4].

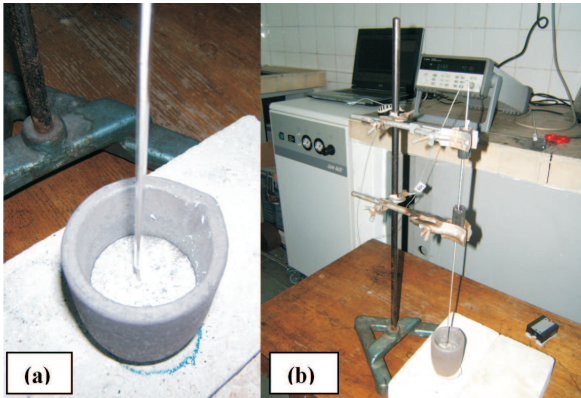


Fig. 1. (a) detail crucible with thermocouple, (b) crucible with thermocouple, data acquisition unit and computer for thermal analysis

### Determination of Grain Size

The determination of the grain size was performed at the Chair of Casting Research, MU Leoben. The casted samples were cut and prepared for the examination. The samples were grinded, polished and etched electrochemically with Barker's reagent. The samples were examined with the LM Zeiss Axio Imager.A1m and the grain size was determined by measuring the real grains with the software NIS Elements Br 3.0, Nikon.

### Scanning Electron Microscopy

Investigations using by SEM were performed at the Chair of Casting Research, MU Leoben. The as-cast samples were investigated by SEM. The samples were studied with a SEM FEI Quanta 200 Mk2 (dual beam) with an acceleration voltage of 20kV. Energy dispersive X-rays (EDX Inca Energy 200, Oxford Instrument) were used for element analysis.

## 3. Results and Discussion

### Thermal analysis

Table 1 shows the results for the undercoolings for various alloys. The initial AlZn20 alloy solidifies with a high undercooling (2.33 K) at the liquidus temperature. The AlZn20+TiBAI, AlZn20+TiCAI and AlZn20+AlZnTi3 alloys show no any or rather a very small (0.21 and 0.56 K) undercooling. The undercooling of AlZn20+AlZnTi3 is moderate (0.56 K).

TABLE 1  
Undercoolings of liquidus temperatures

Alloy	Thermocouple Nr.	Undercooling $\Delta T$ [K]
AlZn20	102	2.33
AlZn20+TiBAI	103	0.00
AlZn20+TiCAI	105	0.21
AlZn20+ZnTi4	107	2.00
AlZn20+AlZnTi3	109	0.56

Table 2 summarises the initial temperatures of primary nucleation (thermal analysis curves are in Figure 2). It is noticeable that  $T_n$  for AlZn20+AlZnTi3 is smaller than  $T_n$  for AlZn20 without grain refinement. A reason for this is the lower melting temperature of the alloy due to the big amount of Zn in the grain refiner (see Table 3, which shows the melting temperatures  $T_m$  for the alloys). AlZn20+TiBAI and AlZn20+TiCAI-alloy show a higher  $T_m$  (627°C), AlZn20 and AlZn20+AlZnTi3-alloy show a lower  $T_m$  (625°C).

TABLE 2  
Initial temperatures of primary nucleation

Alloy	Initial temperature of nucleation $T_n$ [°C]
AlZn20	621.5
AlZn20+TiBAI	628.5
AlZn20+TiCAI	627.0
AlZn20+AlZnTi3	620.5

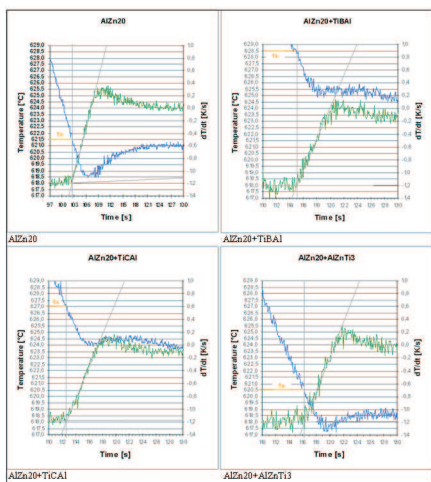


Fig. 2. Detailed liquid temperature thermal analysis (blue) and differentiated thermal analysis (green), showing undercooling and temperature of initial nucleation  $T_n$

TABLE 3

Melting temperatures  $T_m$  calculated with ThermoCalc Classic V3

Alloy	Melting temperature $T_m$ [°C]
AlZn20	625
AlZn20+TiBAI	627
AlZn20+TiCAI	627
AlZn20+AlZnTi3	625

### Grain Size

Table 4 shows the relevant results of the grain size examination. The EqDiameter represents the average grain size. EqDiameter is the calculated average diameter of all detected grains. Figure 3a demonstrates the correlation between used grain refiner and grain size. Figures 3b illustrates in detail representative areas for grain size examination of every alloy. The different scale bars must be noted.

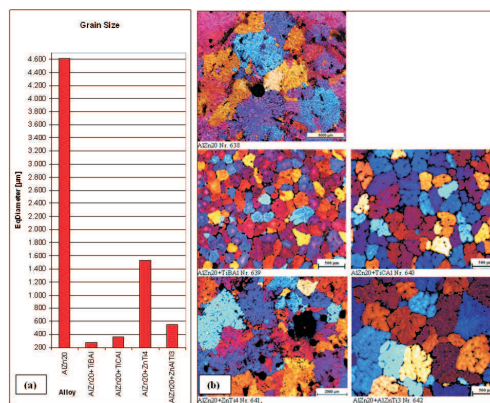


Fig. 3. (a) Diagram showing dependence of grain size on used grain refiner; (b) Micrographs, etched with Baker's

### Scanning Electron Microscope

The results obtained for the different alloys are summarized in the subsequent paragraphs.

Sample AlZn20: Numerous shrinkage porosities were found (see Figure 4a). The matrix shows different concentrations of Zn in Al due to segregation phenomena; see also Figure 4a which is backscatter detection mode BSD. The bright regions at grain boundaries and dendrite interfaces correspond to high concentrations of Zn. A moderate number of inclusions were found which consist of the Al, Zn and Si elements (see Figure 4b spectrum location).

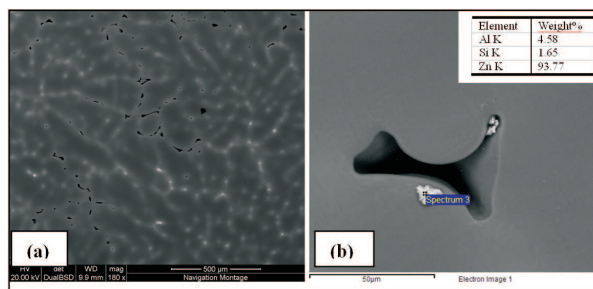


Fig. 4. REM, (a) AlZn20, BSD-mode, overview microstructure with pores, (b) AlZn20, EDX analysis Al-Zn-Si-inclusion

TABLE 4

Results of grain size examination

Sample Nr.	Alloy	EqDiameter [µm]	Area [µm <sup>2</sup> ]	Perimeter [µm]	Length [µm]	Width [µm]	Circularity [-]
638	AlZn20	4.610	17.710.476	19.190	–	–	–
639	AlZn20+TiBAI	275	61.025	1.103	404	154	0,65
640	AlZn20+TiCAI	360	104.599	1.503	564	189	0,61
641	AlZn20+ZnTi4	1.536	1.967.063	10.525	4.822	441	0,30
642	AlZn20+ZnAlTi3	549	244.988	2.447	1.030	227	0,48

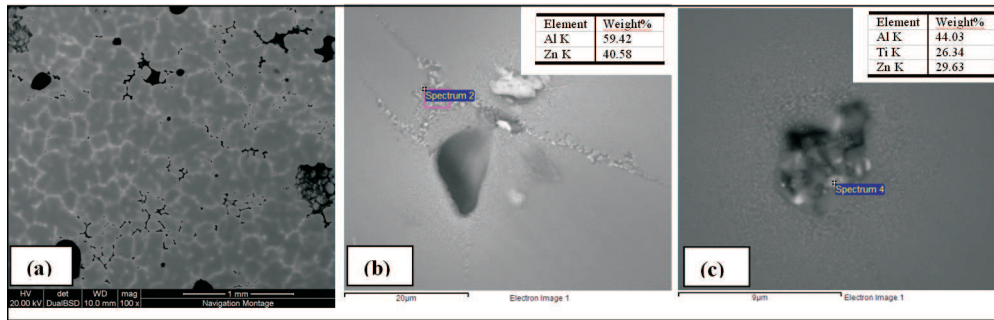


Fig. 5. REM, (a) AlZn20+TiBAI, BSD-mode, overview microstructure with pores, (b) AlZn20+TiBAI, EDX analysis Al-Zn-phase, (c) AlZn20+TiBAI, EDX analysis Ti-Al-Zn-inclusion

Sample AlZn20+TiBAI: Numerous shrinkage and gas porosities were found (see Figure 5a). The matrix shows different concentrations of Zn in Al. A large number of inclusions were found which can be divided into 3 groups:

- inclusions which consists of Al, Zn (and Si) (see Figure 5b)
- inclusions which consists of Al, Zn, Ti (and other elements) (see Figure 5c spectrum location)
- inclusions which consists of Al, Zn and Pb

Sample AlZn20+TiCAI: Numerous shrinkage and gas porosities were found. The matrix shows different concentrations of Zn in Al. A large number of inclusions were found which can be divided into 2 groups:

- inclusions which consists of Al, Zn (and Si)
- inclusions which consists of Al, Zn and Si and/or Fe

Sample AlZn20+AlZnTi4: Numerous shrinkage and gas porosities were found. The matrix shows different concentrations of Zn in Al. A large number of inclusions were found which can be divided into 3 groups:

- inclusions which consists of Al, Zn (and Si)
- inclusions which consists of Al, Zn, Si, Ni (and Fe) (see Figure 6a spectrum location)
- inclusions which consists of Al, Zn and Pb (see Figure 6b spectrum location)

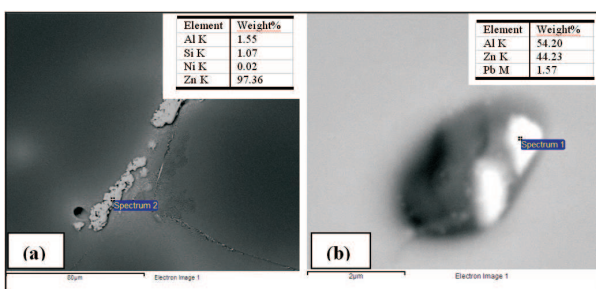


Fig. 6. REM, (a) AlZn20+ZnAlTi3, EDX analysis Al-Zn-Si-Ni-inclusion, (b) AlZn20+ZnAlTi3, EDX analysis Al-Zn-Pb-inclusion

Sample AlZn20+AlZnTi3: Numerous shrinkage porosities were found. The matrix shows different

concentrations of Zn in the Al. A large number of inclusions were found which can be divided into 2 groups:

- inclusions which consists of Al, Zn (and Si)
- inclusions which consists of Al, Zn, Si, Ni (and Fe)

#### 4. Summary

Microstructural features of AlZn20-alloys were analyzed by various examinations. The investigations show that the used grain refiners have a strong influence to microstructure.

The observed large magnitude grain size (4610  $\mu\text{m}$ ) of the initial AlZn20 alloy requires performing the inoculation process. The thermal analysis shows that not enough nuclei are active in the melted initial alloy ( $\Delta T$  2,33 K) and this leads to a high undercooling. The smallest grain size (275  $\mu\text{m}$ ) and the minimal undercooling ( $\Delta T$  0 K) are obtained at AlZn20+TiBAI, AlZn20+TiCAI and this shows a small grain size (360  $\mu\text{m}$ ) and undercooling ( $\Delta T$  0,21 K), as well as AlZn20+ZnAlTi3 (549  $\mu\text{m}$  and  $\Delta T$  0,56 K). AlZn20+ZnTi4 shows moderate grain size (1536  $\mu\text{m}$ ) and high undercooling ( $\Delta T$  2,00 K).

The onset of the primary nucleation temperature  $T_n$  increases for the grain refined samples AlZn20+TiBAI and AlZn20+TiCAI in comparison with the initial alloy AlZn20. On the other hand, the alloy AlZn20+AlZnTi3 does not show any increase of the  $T_n$  temperature, though the AlZn-Ti3 master alloy causes also grain-refinement of the AlZn20 alloy. Elucidation of this requires performing additional, more detail examinations. The microstructures of all the samples show numerous shrinkage porosities. Furthermore, the samples of the alloys AlZn20+TiBAI, AlZn20+TiCAI, AlZn20+ZnTi4 show numerous gas porosities. Although the samples consist of high purity material components, inclusions of the particles containing Si and Pb were found.

### Acknowledgements

The authors would like to acknowledge the European Commission for funding this study which is a part of the Marie Curie TOK-DEV programme, contract no. MTKD-CT-2006-042468 (CastModel).

### REFERENCES

[1] 42<sup>nd</sup> Census of World Casting Production – 2008, *Modern Casting*, **12**, 18-19 (2009).

- [2] K. Haberl, Examination of AlZn20 alloyed with various grain refiners, Report Marie Curie Host Fellowship, July 2009, University of Leoben, Austria, **4-7**, 11-12 (2009)(unpublished).
- [3] S. Nafisi, R. Ghomashchi, *Journal of Materials Processing Technology*, **174**, 371-383 (2006).
- [4] L. Gao, S. Liang, R. Chen, E. Han, *Transaction of Nonferrous Metals Society of China* (Dec. **18**, Supplement 1, 288-291 2008).
- [5] W. K. Krajewski, J. Buraś, M. Żurkowski, A.L. Greer, *Archives of Metallurgy and Materials*, **54**, 329-334 (2009).

*Received: 10 February 2010.*